



Magnetohydrodynamic Stability of Jeffery-Hamel Flow using Different Nanoparticles

M. D. S. Alam^{1†}, M. A. H. Khan², M. A. Alim²

¹*Department of Mathematics, Jagannath University, Dhaka-1100, Bangladesh*

²*Department of Mathematics, Bangladesh University of Engineering and Technology, Dhaka-1000, Bangladesh*

†*Corresponding Author Email: sarwardu75@gmail.com, sarwar@math.jnu.ac.bd,*

(Received December 14, 2014; accepted February 5, 2015)

ABSTRACT

The effects of three different nanoparticles and magnetic field on the nonlinear Jeffery-Hamel flow of water based nanofluid are analyzed in the present study. The basic dimensionless governing equations are solved using series solution which are then analysed to inspect the instability of the problem by a semi-numerical analytical technique called Hermite- Padé approximation. The velocity profiles are presented in convergent-divergent channels for various values of nanoparticles solid volume fraction, Hartmann number, Reynolds number and channel angle. The dominating singularity behavior of the problem is analysed numerically and graphically. The critical relationships among the parameters are also performed qualitatively to observe the behavior of the various nanoparticles.

Keywords: Jeffery-Hamel flow; Magnetohydrodynamic; Nanofluid; Dominating singularity; Hermite-Padé approximation.

NOMENCLATURE

f	base fluid	α	channel angle
H	Hartmann number	ϕ	nanoparticles volume fraction
Re	Reynolds number	μ	dynamic viscosity
s	nano-solid particle	ν	kinematic viscosity
nf	nanofluid	ρ	density
		θ	any angle
		η	dimensionless angle

1. INTRODUCTION

The study of flows in converging-diverging channel is very important due to its industrial, aerospace, chemical, civil, environmental, mechanical and bio- mechanical engineering applications. Various applications of this type of mathematical model are to understand the flow of rivers and canals and the blood flow in the human body. Jeffery (1915) and Hamel (1916) first studied the two-dimensional steady motion of a viscous fluid through convergent-divergent channels which is called classical Jeffery-Hamel flow in fluid dynamics. Jeffery-Hamel flows are interesting models of the phenomenon of separation of boundary layers in divergent channels. These flows have discovered similarity solutions of the Navier-Stokes equations depending on two non-dimensional parameters,

the flow Reynolds number and channel angular widths. Fraenkel (1962) then investigated the laminar flow in symmetrical channels with slightly curved walls. In his analysis the velocity field of the flow was obtained as a power series in small curvature parameter where the leading term is the Jeffery-Hamel solution. Sobey and Drazin (1986) studied some instabilities and bifurcations of two-dimensional Jeffery-Hamel flows using analytical, numerical and experimental methods. Moreover, the steady flow of a viscous incompressible fluid in a slightly asymmetrical channel was studied by Makinde (1997). He expanded the solution into a Taylor series with respect to the Reynolds number and performed a bifurcation study. The theory of MHD is inducing current in a moving conductive fluid in the presence of magnetic field; such induced current results force on ions of the conductive fluid. The

theoretical study of MHD channel has been a subject of great interest due to its extensive applications in designing cooling systems with liquid metals, MHD generators, accelerators, pumps, and flow meters in (Cha *et al.* 2002, Tendler 1983). Makinde (2006) investigated the magnetohydrodynamic (MHD) flows in convergent- divergent channels which was an extension of the classical Jeffery-Hamel flows to MHD. He interpreted that the effect of external magnetic field works as a parameter in solution of the MHD flows in convergent - divergent channels. A survey of information on this problem can be found in the Esmaili *et al.* (2008). Recently, the three analytical methods such as Homotopy analysis method, Homotopy perturbation method and Differential transformation method (DTM) were used by Joneidi *et al.* (2010) to find the analytical solution of Jeffery-Hamel flow. Moreover, the models on classical semi-analytical methods have experienced a revival, in connection with the scheme of new hybrid numerical-analytical techniques for nonlinear differential equations, such as Hermite–Padé approximation method, which demonstrated itself as a powerful benchmarking tool and a prospective substitute to traditional numerical techniques in various applications in science and engineering. The classical Jeffery-Hamel problem was extended in Axford (1961) to include the effects of external magnetic field on conducting fluid. Motsa *et al.* (2010) found the solution of the nonlinear equation for the MHD Jeffery-Hamel problem by using spectral-homotopy analysis method. Moghimi *et al.* (2011) also solved the Jeffery-Hamel flow problem by using the homotopy perturbation method. Alam and Khan (2010) studied the critical behavior of the MHD flow in convergent-divergent channels. The convergence of critical values and the change in bifurcation graph for flow Reynolds number and channel angle by the positive effect of H and the critical relationship among the parameters was discussed. Taghikhani (2014) investigated the magnetic field effect on laminar natural convection flow in a filled enclosure with internal heat generation using two-dimensional numerical simulation and showed that the strength of the magnetic field has significant effects on the flow and temperature fields. Taking into account the rising demands of modern technology, including chemical production, power station, and microelectronics, there is a need to develop new types of fluids that will be more effective in terms of heat exchange performance. The term ‘nanofluid’ was envisioned to describe a fluid in which nanometer-sized particles were suspended in conventional heat transfer basic fluids in Kaka and Pramuanjaroenkij (2009). The effects of magnetic field and nanoparticle on the Jeffery-Hamel flow using Adomian decomposition method were studied by Sheikholeslami *et al.* (2012). The velocity inside the divergent channel for different values of Hartmann number and channel angle and the effect of nanoparticle volume fraction on velocity field in absence of magnetic field was shown in

their analysis. More recently, Moradi *et al.* (2013) investigate the effect of three types of nanoparticles Cu, TiO₂ and Al₂O₃ on Jeffery-Hamel flow using Differential Transformation Method (DTM). They found that the influence of solid volume fraction of nanoparticles on the velocity and skin friction was more enunciated when compared with the type of nanoparticles. Also, the skin friction coefficient for Al₂O₃ was observed maximum in comparison to the other two nanoparticles.

The aim of this work is to find the approximate solutions to the MHD Jeffery-Hamel flow using nanofluid by algebraic programming language MAPLE. The series is analysed by using Hermite–Padé approximation to show the velocity profiles with effect of ϕ , α and Hartmann number H . The critical values and bifurcation diagrams of channel angle and flow Reynolds number with the effect of ϕ for Cu, TiO₂, Al₂O₃ -nanoparticles are studied numerically and graphically. The critical relationships among the parameters are also shown which is not addressed yet.

2. MATHEMATICAL FORMULATION

Consider a steady two-dimensional laminar incompressible viscous nanofluid flow from a source or sink between two channel walls intersect at an angle 2α . A cylindrical coordinate system (r, θ, z) is used and assume that the velocity is purely radial and depends on r and θ so that there is no change in the flow parameter along the z -direction. Further it is presumed that there is an external magnetic field acting vertically downward to the top wall. Let α be the semi-angle and the domain of the flow be $-\alpha < \theta < \alpha$. Then the governing equations for the flow can be expressed as

$$\frac{\rho_{nf}}{r} \frac{\partial}{\partial r}(ru) + \frac{\rho_{nf}}{r} \frac{\partial}{\partial \theta}(rv) = 0, \quad (1)$$

$$u \frac{\partial u}{\partial r} + \frac{v}{r} \frac{\partial u}{\partial \theta} - \frac{v^2}{r} = -\frac{1}{\rho_{nf}} \frac{\partial p}{\partial r} + v_{nf} \left(\nabla^2 u - \frac{u}{r^2} - \frac{2}{r^2} \frac{\partial v}{\partial \theta} \right) - \frac{\sigma B_0^2}{\rho_{nf} r^2} u, \quad (2)$$

$$u \frac{\partial v}{\partial r} + \frac{v}{r} \frac{\partial v}{\partial \theta} + \frac{uv}{r} = -\frac{1}{\rho_{nf} r} \frac{\partial p}{\partial \theta} + v_{nf} \left(\nabla^2 v - \frac{v}{r^2} \right) + \frac{2}{r^2} \frac{\partial u}{\partial \theta}, \quad (3)$$

$$\text{Where } \nabla^2 = \frac{\partial^2}{\partial r^2} + \frac{1}{r} \frac{\partial}{\partial r} + \frac{1}{r^2} \frac{\partial^2}{\partial \theta^2}$$

Assume a symmetric radial flow, so that $v=0$. Also the volumetric flow rate through the channel is

$$Q = \int_{-\alpha}^{\alpha} ur d\theta \tag{4}$$

The boundary conditions are

$$u = 0 \quad \text{at} \quad \theta = \pm\alpha$$

Where B_0 is the electromagnetic induction, σ is the conductivity of the fluid, u is the velocity along radial direction and p is the fluid pressure. The effective density ρ_{nf} , the effective dynamic viscosity μ_{nf} , and the kinematic viscosity ν_{nf} of the nanofluid are given as Aminossadati and Ghasemi (2009).

$$\begin{aligned} \rho_{nf} &= \rho_f(1-\phi) + \rho_s\phi, \\ \mu_{nf} &= \frac{\mu_f}{(1-\phi)^{2.5}}, \quad \nu_{nf} = \frac{\mu_{nf}}{\rho_{nf}} \end{aligned} \tag{5}$$

Here, ϕ is the solid volume fraction of the nanoparticles.

If it requires $Q \geq 0$, then for $\alpha > 0$ the flow is diverging to a source at $r = 0$.

Let $\psi = \psi(r, \theta)$ be the stream function, then

$$\partial\psi/\partial\theta = ur, \quad \partial\psi/\partial r = 0$$

Introducing the dimensionless variables

$$\eta = \theta/\alpha \quad \text{and} \quad F(\eta; Re, H, \phi, \alpha) = \psi(\theta)/Q,$$

The Navier-Stokes equations (1-3) reduce to the ordinary differential equation

$$\begin{aligned} F^{(iv)} + 2\alpha ReA(1-\phi)^{2.5} FF'' \\ + (4 - (1-\phi)^{1.25}H)\alpha^2 F'' = 0 \end{aligned} \tag{6}$$

The boundary conditions are as follows:

$$F = \pm 1, \quad F' = 0 \quad \text{at} \quad \eta = \pm 1 \tag{7}$$

$$\begin{aligned} A &= (1-\phi) + \frac{\rho_s}{\rho_f}\phi, \\ Re &= \frac{Q}{\nu_f}, \quad H = \sqrt{\frac{\sigma B_0^2}{\rho_f \nu_f}} \end{aligned} \tag{8}$$

Where A is a parameter, Hartmann number H , flow Reynolds number Re , channel angle α and nanoparticles solid volume fraction ϕ .

3. SERIES ANALYSIS

The following power series expansion is considered in terms of the parameter α as equation (6) is non-linear for velocity field

$$F(\eta) = \sum_{i=0}^{\infty} F_i(\eta)\alpha^i, \quad \text{as} \quad |\alpha| < 1 \tag{9}$$

The non-dimensional governing equations are then solved into series solution by substituting the Eq.

(9) into Eqs. (6) and (7) and equating the coefficients of powers of α .

Order zero (α^0):

$$\frac{d^4 F_0(\eta)}{d\eta^4} = 0, \tag{10}$$

$$F_0(\pm 1) = \pm 1, \quad F_0'(\pm 1) = 0, \tag{11}$$

Order one (α^1):

$$\begin{aligned} \frac{d^4 F_1(\eta)}{d\eta^4} + 2 ReA(1-\phi)^{2.5} \frac{dF_0(\eta)}{d\eta} \frac{d^2 F_0(\eta)}{d\eta^2} = 0 \\ F_1(\pm 1) = 0, \quad F_1'(\pm 1) = 0, \end{aligned} \tag{12}$$

$$F_1(\pm 1) = 0, \quad F_1'(\pm 1) = 0, \tag{13}$$

With the help of MAPLE, we have computed the first 18 coefficients for the series of the velocity $F(\eta)$ in terms of α, H, Re, ϕ, A . The first few coefficients of the series for $F(\eta)$ are as follows:

$$\begin{aligned} F(\eta; \alpha, Re, H, \phi, A) &= \frac{3}{2}\eta - \frac{1}{2}\eta^3 - \frac{3}{280}Re \\ &A(1-\phi)^{(5/2)}\eta(\eta^2-5)(\eta-1)^2(\eta+1)^2\alpha \\ &+ \frac{1}{431200}\eta(\eta-1)^2(\eta+1)^2(43120+9590\eta^4 \\ &Re^2 A^2 \phi^2 - 9590\eta^4 Re^2 A^2 \phi^3 \\ &+ 4795\eta^4 Re^2 A^2 \phi^4 - 959\eta^4 Re^2 A^2 \phi^5 \\ &- 4795\eta^4 Re^2 A^2 \phi - 24720\eta^2 Re^2 A^2 \phi^2 \\ &+ 24720\eta^2 \\ &Re^2 A^2 \phi^3 - 12360\eta^2 Re^2 A^2 \phi^4 \\ &+ 2472\eta^2 Re^2 A^2 \phi^5 + 12360\eta^2 Re^2 A^2 \phi \\ &- 980\eta^6 Re^2 A^2 \phi^2 + 980\eta^6 Re^2 A^2 \phi^3 \\ &- 490\eta^6 Re^2 A^2 \phi^4 + 98\eta^6 Re^2 A^2 \phi^5 \\ &+ 490\eta^6 Re^2 A^2 \phi + 2875 Re^2 A^2 \\ &- 10780H(1-\phi)^{(1/4)} + 28750 Re^2 A^2 \phi^2 \\ &- 28750 Re^2 A^2 \phi^3 - 98\eta^6 Re^2 A^2 \\ &- 2472\eta^2 Re^2 A^2 + 959\eta^4 Re^2 A^2 \\ &+ 10780H(1-\phi)^{(1/4)} \\ &\phi - 2875 Re^2 A^2 \phi^5 - 14375 Re^2 A^2 \phi \\ &+ 14375 Re^2 A^2 \phi^4)\alpha^2 + O(\alpha^3) \dots \end{aligned} \tag{14}$$

Applying differential and algebraic approximate methods to the series we determine the comparison between the present and previous solutions and the convergence of critical values and the changes in bifurcation graphs for the channel angle and flow Reynolds number by the positive effect of nanoparticle volume fraction. The effect of magnetic field and nanofluid on velocity field are also shown graphically using differential

approximate method. The details of Hermite-Padé approximants method are described below.

4. COMPUTATIONAL PROCEDURE: HERMITE-PADÉ APPROXIMANTS.

The idea of channel angle criticality or non-existence of steady-state solution to nonlinear boundary layer equations for certain parameter values are extremely important from physical point of view. To compute the criticality conditions in the system, we shall employ a very efficient solution method, known as Hermite-Padé approximants, which was first introduced by Padé (1892) and Hermite (1893).

Assume that the partial sum

$$S_{N-1}(\alpha) = \sum_{n=0}^{N-1} a_n \alpha^n \quad \text{as } |\alpha| < 1 \quad (15)$$

Because of the continuation of analytical solution and dominating singularity behavior, the bifurcation study is performed using the partial sum (15). The dominating behavior of the function $S(\alpha)$ represented by a series may be written as

$$S(\alpha) \sim \begin{cases} B + A \left(1 - \frac{\alpha}{\alpha_c}\right)^\delta & \text{when } \delta \neq 0, 1, 2, \dots, \\ B + A \left(1 - \frac{\alpha}{\alpha_c}\right)^\delta \ln \left|1 - \frac{\alpha}{\alpha_c}\right| & \text{when } \delta = 0, 1, 2, \dots, \end{cases} \quad (16)$$

as $\alpha \rightarrow \alpha_c$, where A and B are some constants and α_c is the critical point with the critical exponent δ .

Assume that the $(d+1)$ tuple of polynomials, where d is a positive integer:

$$P_N^{[0]}, P_N^{[1]}, \dots, P_N^{[d]}$$

$$\text{where, } \deg P_N^{[0]} + \deg P_N^{[1]} + \dots + \deg P_N^{[d]} + d = N, \quad (17)$$

is a Hermite-Padé form of these series if

$$\sum_{i=0}^d P_N^{[i]}(\alpha) S_i(\alpha) = O(\alpha^N) \quad \text{as } |\alpha| < 1 \quad (18)$$

Here $S_0(\alpha), S_1(\alpha), \dots, S_d(\alpha)$ may be independent series or different form of a unique series. We need to find the polynomials $P_N^{[i]}$ that satisfy the equations (17) and (18). These polynomials are completely determined by their coefficients. So, the total number of unknowns in equation (18) is

$$\sum_{i=0}^d \deg P_N^{[i]} + d + 1 = N + 1 \quad (19)$$

Expanding the left hand side of equation (18) in

powers of α and equating the first N equations of the system equal to zero, we get a system of linear homogeneous equations. To calculate the coefficients of the Hermite-Padé polynomials it requires some sort of normalization, such as

$$P_N^{[i]}(0) = 1 \quad \text{for some integer } 0 \leq i \leq d \quad (20)$$

It is important to emphasize that the only input required for the calculation of the Hermite-Padé polynomials are the first N coefficients of the series $S_0(\alpha), S_1(\alpha), \dots, S_d(\alpha)$. The equation (19) simply ensures that the coefficient matrix associated with the system is square. One way to construct the Hermite-Padé polynomials is to solve the system of linear equations by any standard method such as Gaussian elimination or Gauss-Jordan elimination. In practice, one usually finds that the dominant singularities as well as the possibility of multiple solution branches for the nonlinear problem are located at zeroes of the leading polynomial $P_N^{[d]}(\alpha)$ coefficients of the equation (18). If the singularity is of algebraic type, then the exponent δ may be approximated by

$$\delta_N = d - 2 - \frac{P_N^{[d-1]}(\alpha_{c,N})}{DP_N^{[d]}(\alpha_{c,N})} \quad (21)$$

Drazin –Tourigney (1996) Approximants is a particular kind of algebraic approximants and Khan (2002) introduced High-order differential approximant (HODA) as a special type of differential approximants. High-order partial differential approximants (HPDA) discussed in Rahman (2004) is a partial differential approximants. More information about the above mentioned approximants can be found in the respective references.

5. RESULTS AND DISCUSSION

The main objective of the current work is to analyze the effects of different nanoparticles and magnetic field on Jeffery-Hamel flow of viscous incompressible fluid by using Hermite-Padé approximants. The understanding of the flow physics is achieved through a combination of numerical studies. Although there are four parameters of interest in the present problem the effects of nanoparticles volume fraction ϕ , channel angle α , Reynolds number Re and Hartman number H . The densities of the base fluid, Cu, $\text{TiO}_2, \text{Al}_2\text{O}_3$ -nanoparticles are respectively 998.1 (kg/m^3), 8933 (kg/m^3), 4250 (kg/m^3), 3970 (kg/m^3). The series (14) is analyzed by differential approximation method to show the comparison between present results and the results of Fraenkel (1962) in Tables 1-2 and the variation in the critical values α_c and Re_c with critical exponent β_c for various values of nanoparticles significantly. The results of the numerical

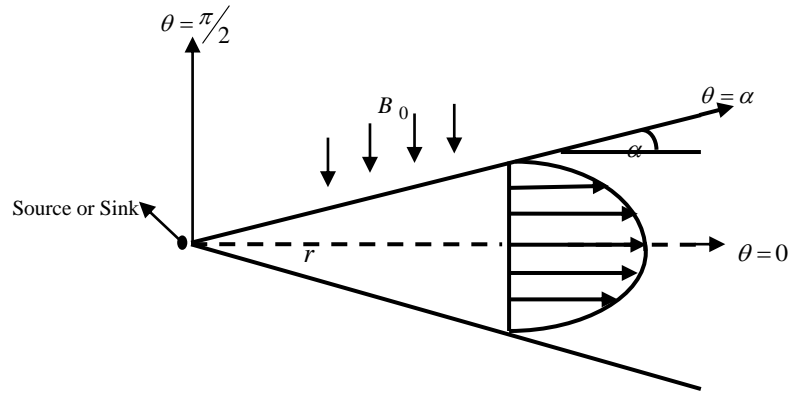


Fig. 1. Geometry of the problem.

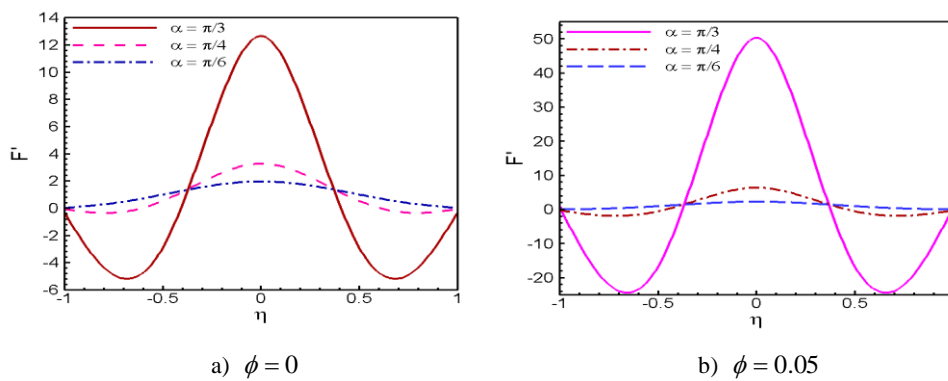


Fig. 2. Velocity profiles in divergent channel with different values of α at $Re = 7, H = 1$ for Cu-water nanofluid.

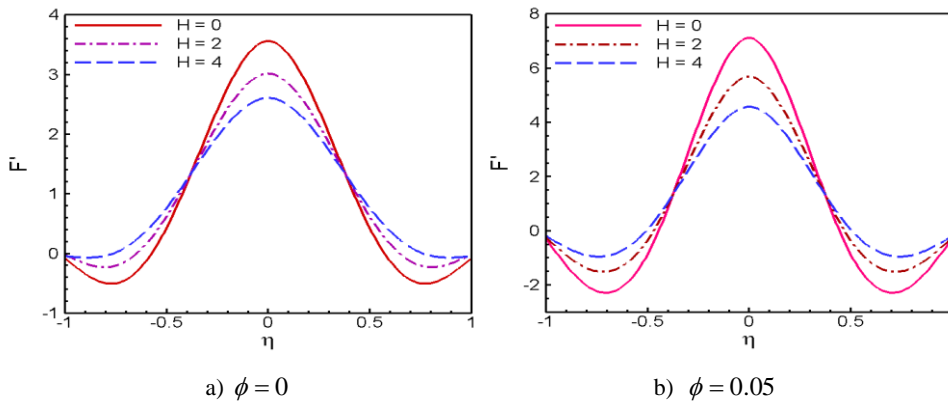


Fig. 3. Velocity profiles in divergent channel with different values of H at $Re = 7, \alpha = \pi/4$ for Cu-water nanofluid.

computations of velocity profiles for different values of the aforementioned parameters are displayed graphically in Figs. (2) - (5).

Table 1 exhibits the changes of critical channel semi-angle α_c for four different values of $\phi = 0, 0.05, 0.1, 0.2$ as Cu-nanoparticles where water is the base fluid at $d = 4$ taking $N = 18$.

The values of δ_c confirm that α_c is a branch point using HODA.

Moreover, Table 2 implies that Re_c decreases both significantly and uniformly for different values of ϕ and Re_c is a branch point verified by the values of δ_c . The results of Tables 1-2 show a good agreement with those results of Fraenkel (1962)

Table 1 Numerical values of critical angles α_c and corresponding exponent δ_c at $Re = 20$ and $H = 1$ for Cu-nanoparticles with various values of ϕ .

	Present study		Fraenkel (1962)
ϕ	α_c	δ_c	α_c
0	0.2691819115000	0.49515872313	0.269
0.05	0.2122678984825	0.49785814583	—
0.1	0.1963360739593	0.50387522948	—
0.2	0.1828175409234	0.49803815751	—

Table 2 Numerical values of critical Re_c and corresponding exponent δ_c at $\alpha = 0.1$ and $H = 1$ for Cu-nanoparticles with various values of ϕ .

	Present study		Fraenkel (1962)
ϕ	Re_c	δ_c	Re_c
0	54.47285679258	0.5071160433	54.61
0.05	44.31499529952	0.4985570114	—
0.1	39.49239826450	0.4996886803	—
0.2	36.73956809792	0.4990504907	—

Table 3 Variation of critical angles α_c with different nanoparticles at $Re = 20$ and $H = 1$ for various values of ϕ .

α_c			
ϕ	Cu	TiO ₂	Al ₂ O ₃
0	0.26918191150	0.2691819115000	0.26918191150
0.05	0.21993061586	0.2632195331417	0.26618826894
0.1	0.19633607395	0.2641976761310	0.26975026485
0.2	0.18281754092	0.2839251923510	0.29355796430

Table 4 Variation of critical Re_c with different nanoparticles at $\alpha = 0.1$ and $H = 1$ for various values of ϕ .

Re_c			
ϕ	Cu	TiO ₂	Al ₂ O ₃
0	54.47285679	54.4728567925	54.47285679
0.05	44.31499529	53.2537722229	53.90465402
0.1	39.49239826	53.4686730461	54.60503673
0.2	36.73956809	57.6132508744	59.63881039

for $\phi = 0$. It is seen from Table 3 that the values of α_c increases uniformly for Cu, TiO₂ and Al₂O₃ nanoparticles respectively as the nanoparticles are arranged in descending order of density. The similar behavior of the above three nanoparticles are observed in Table 4 for critical Reynolds number Re_c .

Figs 2 and 3 show the effects of channel angle and magnetic field on the velocity profiles in divergent channel for both viscous and Cu-water nanofluid respectively. It is seen from Fig 2(a) that the velocity increases moderately with rising values of α at $Re = 7, H = 1$ for viscous fluid ($\phi = 0$) but the differences between velocity profiles are more noticeable at larger angles. However, the backflow is detected in diverging channel for higher values

of $\alpha = \pi/3$. In Fig 2(b) the effect of ($\phi = 0.05$) accelerates the increment of centerline velocities more rapidly and there occur major backflow near the walls at large value of $\alpha = \pi/3$. The flow breaks the symmetry, with most of the fluid going in a thin layer along the walls. The fluid is prevented from utilizing the whole area of the expanding channel by a recirculation vortex which blocks the exit. In addition, secondary instabilities driven by this vertical motion develop in this flow.

The velocity curves in Fig 3(a) show that the rate of alteration is significantly and uniformly reduced with increase of Hartmann number H in absence of Cu-nanoparticles ($\phi = 0$). The transverse magnetic field opposes the alteration phenomena clearly. Because the variation of H leads to the variation of the Lorentz force due to magnetic field and the

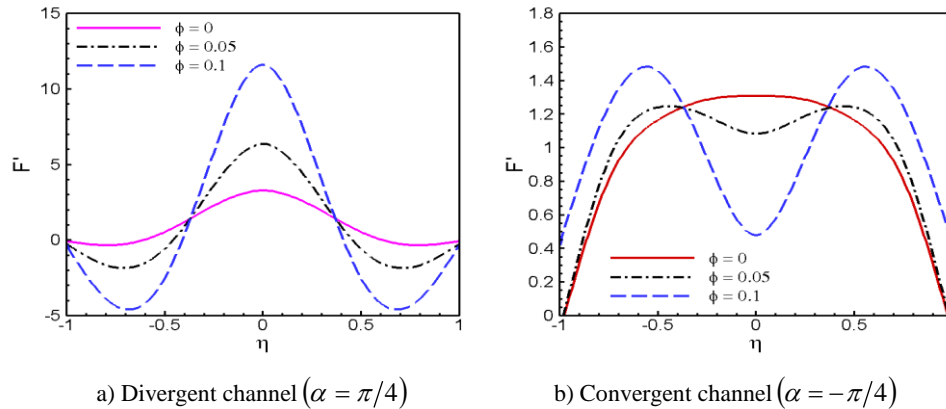


Fig. 4. Velocity profiles with different values of ϕ at $Re = 7, H = 1$ for Cu-water nanofluid.

Lorentz force produces more resistance to the alternation phenomena. It can be noted from Fig 3(b) that the centerline velocity increases reasonably for nanofluid ($\phi = 0.05$) than viscous fluid with dropping H at a small angle $\alpha = 0.1$. Whereas to diminish the backflow an increased H is essential. Fig 4 represents the consequences of solid volume fraction on velocity profile at $\alpha = 0.1$ in both convergent-divergent channels. In Fig. 4(a) at $\alpha = \pi/4$ for divergent channel as ϕ increases, the center line velocity increases and backflow is observed near the walls. Conversely, Fig. 4(b) for convergent channel ($\alpha = -\pi/4$) represents that backflow starts at the centerline when ($\phi = 0.05$) whether there is no sign of backflow in absence of nanoparticles ($\phi = 0$) and this properties is enhanced with rising $\phi = 0.1$. Therefore, the state of backflow in convergent channel is completely opposite in comparison to divergent channel.

Figure 5 predicts the combined effects of magnetic field and Cu-nanoparticles volume fraction on the velocity for divergent channel with fixed Reynolds number. The figure represents sensible decreases in the centerline velocity with rising Hartmann number for both viscous and nanofluid that coincide with those results of Sheikholeslami (2012). It is also observed that for all values of Hartmann number there is no backflow in the viscous fluid ($\phi = 0$), nevertheless backflow starts for nanofluid with $H = 0$ at $\alpha = 0.1, Re = 7$ and this phenomenon is abolished with the rising values of Hartmann number. Employing the algebraic approximation method to the series (14) we have obtained the bifurcation graphs of α and Re . Figure 6(a) shows the bifurcation diagram of α with the effect of nanofluid. It is interesting to notice that there are two solution branches of velocity when $\alpha < \alpha_c$, one solution when $\alpha = \alpha_c$, and no solution when $\alpha > \alpha_c$, where α_c is the critical value of α for

which the solution exists. It can be also noted here that the bifurcation points change from $\alpha \approx 0.2691819115$ to $\alpha \approx 0.2122678984$ and then to $\alpha \approx 0.1963360739$ for different values of Cu-nanoparticles volume fraction respectively at $Re = 20, H = 1$. On the other hand, it is noticed from Fig. 6(b) that the bifurcation curves of TiO_2 and Al_2O_3 -nanoparticles almost coincide whereas there is a significant variation for Cu-nanoparticles due to their respective densities.

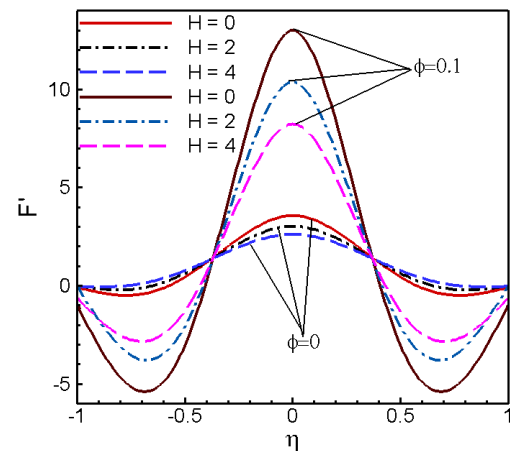


Fig. 5. Combined effects of Hartmann number and solid volume fraction of Cu-nanoparticles on velocity profile for $\alpha = \pi/4, Re = 7$.

Moreover, from Fig 7(a) it is observed that the flow also bifurcates at $Re = Re_c$. On the other hand, the bifurcation points decreases uniformly for three different values of Cu-nanoparticles volume fraction at $\alpha = 0.1, H = 1$. Figure 7(b) represents the effect of three different nanoparticles on the bifurcation diagram of Re remarkably. The conjecture of Figs 6(a-b) and 7(a-b) is consistent with the results shown in Tables 1-4 using differential approximation. One major finding is that, as nanoparticles volume fraction increases the critical channel angle and flow Reynolds number

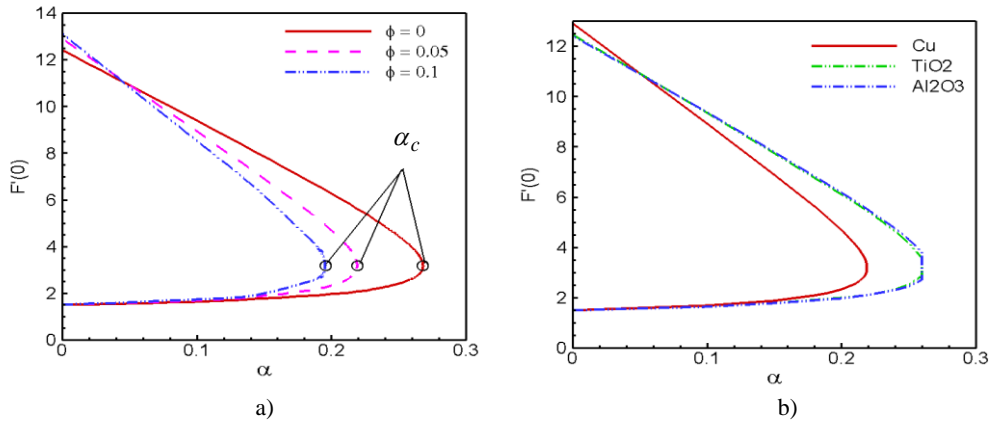


Fig. 6. Approximate bifurcation diagrams of α in the $(\alpha, F'(0))$ plane at $H = 1, Re = 20$ (a) with different ϕ of Cu-water nanofluid and (b) for various types of nanoparticles at $\phi = 0.05$ obtained by Drazin-Tourigny method (1996) for $d = 4$.

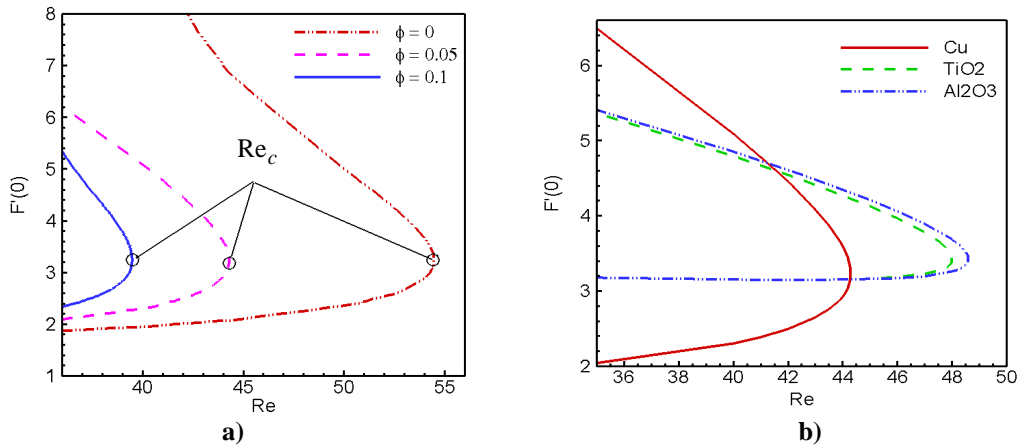


Fig. 7. Approximate bifurcation diagrams of Re in the $(Re, F'(0))$ plane at $H = 1, \alpha = 0.1$ (a) with different ϕ of Cu-water nanofluid and (b) for various types of nanoparticles at $\phi = 0.05$ obtained by Drazin-Tourigny method (1996) for $d = 4$.

decreases. The temporal and spatial complexity of observed flows changes in a succession of bifurcations until the onset of instability. Each bifurcation is marked by the onset of instability of one flow and followed by equilibrium to another stable flow. The High-order partial Differential Approximant HPDA (2004) is applied to the series (14) in order to determine the critical relationship among the parameters α, H and Re with the effect of nanofluid. Fig 8(a) displays the critical relation between the channel angular width α and flow Reynolds number Re for three various values of nanoparticles solid volume fraction. It is found that as α increases then Re decreases and conversely Re increases when α decreases. This implies that both channel angle and Reynolds number are inversely proportional to each other which are an excellent agreement with previously established results obtained by Fraenkel (1962) for $\phi = 0$ in classical Jeffery-Hamel flow. A significant variation is observed in the relationship curves of

Cu-nanoparticles for $\phi = 0.05$ & $\phi = 0.1$.

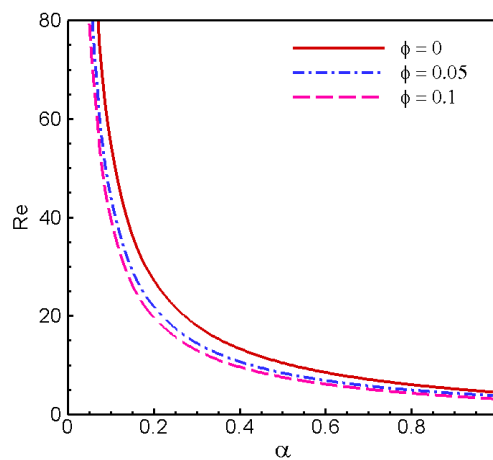


Fig. 8. Critical relation between α and Re with different values of ϕ for Cu-water nanofluid at $H = 1$ obtained by HPDA (2004) for $d = 5$.

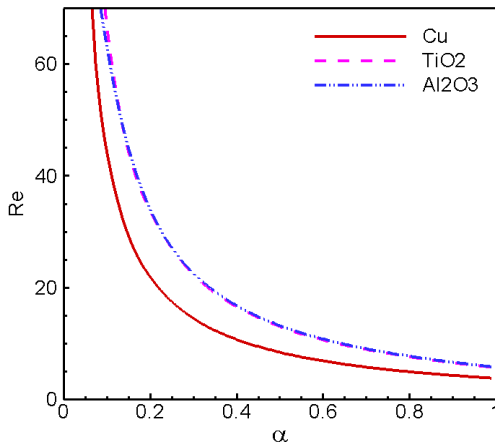


Fig. 9. Critical relation between α and Re for different nanoparticles at $\phi = 0.05$, $H = 1$ obtained by HPDA (2004) for $d = 5$.

Moreover, from Fig. 9 it is found that Cu-nanoparticles produce a clear difference in the relationship curve than TiO_2 and Al_2O_3 - nanoparticles.

Fig.10 depicts the relationship between α and Hartmann number H with different volume fraction of nanoparticles in divergent channel. It is seen from the figure that α increases as H increases and the rate of increment is lower in Cu-water nanofluid.

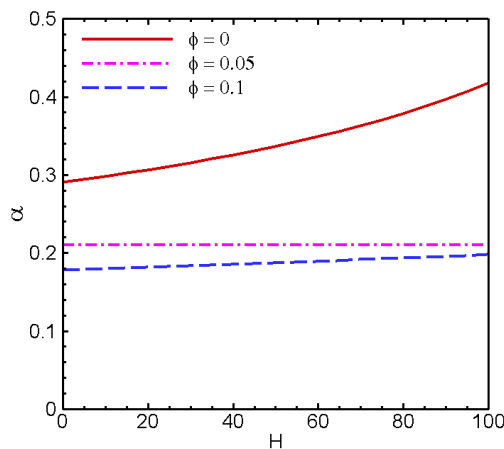


Fig. 10. Critical relation between α and H for different values of ϕ with Cu-water nanofluid at $Re = 20$ obtained by HPDA(2004) for $d = 4$.

However, α decreases as ϕ increases. Finally, in Fig.10, the flow Reynolds number Re increases with rising H but then the tendency of increment becomes slower for $\phi = 0.05$ & $\phi = 0.1$. The conjecture of both the Figs 10 and 11 are coincides with those results of Alam and Khan (2010) at $\phi = 0$. Therefore, nanofluid diminishes the alternation phenomenon in the relationship graphs among the parameters. Series analysis plays an important role in many areas, particularly in fluid dynamics, where, as mentioned earlier, the presence

of real singularities in the solution may reflect some changes in the nature of the flow. The criticality of channel angle and flow Reynolds number lead to instability in the fluid flow with a significant effect of nanofluid.

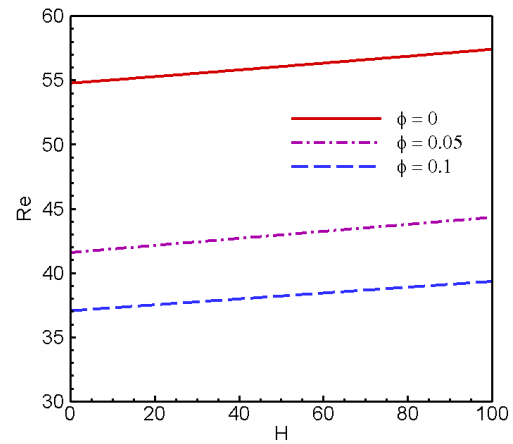


Fig. 11. Critical relation between Re and H for different values of ϕ with Cu-water nanofluid at $\alpha = 0.1$ obtained by HPDA (2004) for $d = 4$.

6. CONCLUSION

The magnetohydrodynamic Jeffery-Hamel flow problem with three types of nanoparticles as water is the base fluid is investigated applying Hermite-Padé approximation technique. A comparison is made between the available results and the present approximate solutions. The accurate numerical approximation of the critical parameters of the flow is obtained. The influence of various physical parameters on the velocity is discussed in detail. The basic conclusions are as follows:

- Increasing channel semi angle leads to enrichment of fluid centerline velocity in the channel.
- Increasing Hartmann number reduces fluid flow in the channel centerline and produces the backflow reduction near the walls for both base fluid and nanofluid.
- The velocity increases as nanoparticles volume fraction increases along the centerline whereas increasing volume fraction generates backflow near the walls.
- The dominating singularity behaviour is a branch point singularity with the critical exponent half for both the wall divergence semi-angle α and flow Reynolds number Re is found with the effect of various types of nanoparticles volume fraction.
- The critical relationship among the parameters with the effect of nanofluid coincides with the conjecture of classical Jeffery-Hamel flow.

Hermite-Padé approximation technique could produce better and accurate results if more terms of the series were computed. However, we provide a basis for guidance about new approximants idea for

summing power series that should be chosen for many problems in fluid mechanics and similar subjects.

ACKNOWLEDGEMENT

This work is done within the framework of the PhD program of the corresponding author under Department of Mathematics, Bangladesh University of Engineering and Technology, Dhaka. Financial support from the Bangabandhu Fellowship on Science and ICT project is acknowledged.

REFERENCES

- Alam, M. S. and M. A. H. Khan (2010). Critical behaviour of the MHD flow in convergent-divergent channels. *Journal of Naval Architecture and Marine Engineering* 7(2), 83 - 93.
- Aminossadati, S. M. and B. Ghasemi (2009). Natural convection cooling of a localized heat source at the bottom of a nanofluid-filled enclosure. *Eur. J. Mech. B/Fluids* 28, 630–640.
- Axford, W. I. (1961). The Magnetohydrodynamic Jeffery–Hamel problem for a weakly conducting fluid. *Q. J. Mech. Appl. Math* 14, 335–351.
- Cha, J. E., Y. C. Ahn and M. H. Kim (2002). Flow measurement with an electromagnetic flow meter in two-phase bubbly and slug flow regimes. *Flow Measurement and Instrumentation* 12(5-6), 329–339.
- Drazin, P. G. and Y. Tourigny (1996). Numerically study of bifurcation by analytic continuation of a function defined by a power series. *SIAM Journal of Applied Mathematics* 56, 1-18.
- Esmaili, Q., A. Ramiar, E. Alizadeh and D. D. Ganji (2008). An approximation of the analytical Solution of the Jeffery–Hamel flow by decomposition method. *Physics Letters A* 372, 3434–3439.
- Fraenkel, L. E. (1962). Laminar flow in symmetrical channels with slightly curved walls. I: On the Jeffery-Hamel solutions for flow between plane walls. *Proceeding of the Royal Society of London* 267, 119-138.
- Hamel, G. (1916). Spiralförmige Bewegungen Zäher Flüssigkeiten, *Jahresbericht der Deutschen Math. Vereinigung* 25, 34-60.
- Hermite, C. (1893). Sur la généralisation des fractions continues algébriques. *Annali di Mathematica Pura e Applicata* 21(2), 289-308.
- Jeffery, G. B. (1915). The two-dimensional steady motion of a viscous fluid. *Philosophical Magazine* 6, 455-465.
- Joneidi, A. A., G. Domairry and M. Babaelahi (2010). Three analytical methods applied to Jeffery–Hamel flow, *Commun. Nonlinear Sci. Numer. Simulat* 15, 3423–3434.
- Kaka, C. S. and A. Pramuanjaroenkij (2009). Review of convective heat transfer enhancement with nanofluids. *International Communications in Heat and Mass Transfer* 52(13-14), 3187-3196.
- Khan, M. A. H. (2002). High-Order Differential Approximants, *Journal of Computational and Applied Mathematics* 149, 457-468.
- Makinde, O. D. (1997). Steady flow in a linearly diverging asymmetrical channel. *Computer Assisted Mechanics and Engineering Sciences* 4, 157-165.
- Makinde, O. D. and P. Y. Mhone (2006). Hermite-Pade' Approximation approach to Hydromagnetic flows in convergent-divergent channels. *Applied Mathematics and Computations* 181(2), 966-972.
- Moghimia, S. M., D. D. Ganji, H. Bararnia, M. Hosseiniand M. Jalaal (2011). Homotopy perturbation method for nonlinear MHD Jeffery–Hamel Problem. *Computers and Mathematics with Applications* 61, 2213-2216.
- Moradi, A., A. Alsaedi and T. Hayat (2013). Investigation of Nanoparticles Effect on the Jeffery-Hamel Flow. *Arab J. Sci. Eng* 38, 2845-2853.
- Motsa, S. S., P. Sibanda, F. G. Awad and S. Shateyi (2010). A new Spectral-Homotopy analysis method for the MHD Jeffery–Hamel problem. *Computers & Fluids*. 39, 1219-1225.
- Padé, H. (1892). Sur la représentation approchée d'une fonction pour des fractions rationnelles. *Ann. Sci. École Norm. Sup. Suppl* 9, 1-93.
- Rahman, M. M. (2004). *A New Approach to Partial Differential Approximants*. M. Phil thesis, Bangladesh University of Engineering & Technology, Dhaka.
- Sheikholeslami, M., D. D. Ganji, H. R. Ashorynejad and H. B. Rokni (2012). Analytical investigation of Jeffery-Hamel flow with high magnetic field and nanoparticle by Adomian decomposition method. *Appl. Math. Mech. Engl. Ed* 33, 25–36.
- Sobey, I. J. and P. G. Drazin (1986). Bifurcations of two-dimensional channel flows. *Journal of Fluid Mechanics* 171, 263-287.
- Taghikhani, M. A. (2015). Magnetic Field Effect on Natural Convection Flow with Internal Heat Generation using Fast $\psi - \Omega$ Method. *Journal of Applied Fluid Mechanics* 8(2), 189-196.
- Tendler, M. (1983). Confinement and related transport in extrap geometry. *Nuclear Instruments and Methods in Physics Research* 207(1-2), 233–240.